We are IntechOpen, the world's leading publisher of Open Access books Built by scientists, for scientists

4,800
Open access books available

122,000
International authors and editors

135M
Downloads

Our authors are among the

154
Countries delivered to

TOP 1%
most cited scientists

12.2%
Contributors from top 500 universities

CLARIVATE ANALYTICS
BOOK CITATION INDEX
INDEXED

WEB OF SCIENCE™

Selection of our books indexed in the Book Citation Index
in Web of Science™ Core Collection (BKCI)

Interested in publishing with us?
Contact book.department@intechopen.com

Numbers displayed above are based on latest data collected.
For more information visit www.intechopen.com

13

Novel Electroless Metal Deposition - Oxidation on Mn – Mn$_x$O$_y$ for Water Remediation

José de Jesús Pérez Bueno[1,*] and Maria Luisa Mendoza López[2]
[1]Centro de Investigación y Desarrollo Tecnológico en Electroquímica,
S.C., Parque Tecnológico Querétaro-Sanfandila,
[2]Instituto Tecnológico de Querétaro, Av. Tecnológico s/n Esq. M. Escobedo Col. Centro
México

1. Introduction

Water pollution not only increases in amount every year but it increases in higher toxic contaminants. Humanity has acquired, with harsh and tragic experience, a consciousness of care for the environment. New laws and norms throughout the world prove this. The quest for new processes, as an alternative to those already in use, has been testing many different physical and chemical procedures.

A conventional procedure for the removal of metal ions is chemical precipitation of hydroxides by adjusting the pH (Zouboulis et al., 2002). During the last decade, zero-valent iron has been used for the removal of metals such as zinc and mercury (Dries et al., 2005; Oh et al., 2007; Noubactep, 2010). This procedure is part of the electroless deposition.

The electroless metal deposition has been used in many industries especially due to polymers metallization. Electroless is comprised into three different procedures; autocatalytic, cementation and galvanic deposition.

The cementation process offers the possibility of removing contaminants from water considering its standard electrode potential according to the electromotive series without an external current. Ions of a relatively nobler element are reduced using electrons in exchange for a less nobler metal that gets oxidized. Usually, this process occurs over the entire surface, which concludes by blocking the deposition. This through that limits the applications of the process.

The cementation process has been used for the removal of gold, e.g., using magnesium. The deposition rate of gold is directly proportional to its initial concentration and time (Kuntyi et al., 2007).

Electroless metal deposition has been used for the synthesis of self-assembling silicon nanowires. In this case, it was assumed that the simultaneous growth of metal dendrites, accompanied with the etching of the silicon wafer, was important for the formation of 1D nanostructures (Peng, 2003).

The quantity of oxide formed on the cementating surface depends on pH, the quantity of the cementation agent and the stir variation. The reactivity of Fe^0 depends on the porosity of the

oxides formed, the water salinity and the nature of the contaminant. A generation of thicker oxides was identified as being beneficial for the removal of contaminants and their potential reaction products can progressively be trapped in the matrix and remain very stable (Noubactep, 2010).

The removal of metallic ions in aqueous solution by zero-valent iron has been studied in research papers during the last decade (Noubactep, 2009). This route is fundamentally a cementation electroless process. It has been identified as having a synergic effect between adsorption, co-precipitation and the reduction of the contaminant on Fe^0/H_2O. Those studies associate metal removal through a combination of adsorption and co-precipitation onto iron corrosion products and reduction by using Fe^0, Fe^{II} or H_2/H.

This work considers the remediation of water by using electroless going through the formation of oxides immediately after the reduction of the metallic specie on the active surface. A high porosity of the deposited oxide may result, but not necessarily, fundamental in the process of forming the deposit.

2. Methodology

This work used standard ions solutions for water remediation evaluation because of the influence of manganese-manganese oxide. Silver nitrate, aluminum nitrate and lead nitrate (JT Baker) were used for the 1000ppm, 500ppm, and 100ppm solutions in deionizer water.

The crystallinity of manganese-manganese oxide substrates (Alfa Aesar, 99%) and that of deposits were characterized by X-ray diffraction (D8 Advance, Bruker AXS). The deposits weights were obtained by weight differences between the deposit-substrate and the substrate.

The pieces of manganese-manganese oxide used as substrates, with weight and area previously measured, were immersed in 50mL of a standard ion solution. The substrates had two different surfaces, one of them flat and the other irregular; for this study, the depositions were always on the flat surfaces.

When each test concluded, the solution was removed carefully with a pipette from the flask were the test were conducted, leaving the deposit-substrate samples untouched. The deposit-substrate samples were dried at room temperatures. The weight of the deposits was determined by weight difference between the deposit-substrate sample and the original substrate.

The characterizations of morphology and microanalysis of deposits and substrate were performed in a scanning electron microscopy (SEM, JEOL model JSM-5400LV) coupled to a microanalysis (EDS, Kevex-TermoNORAN).

The absorbance and reflectance studies of deposits were determined by Ocean Optics –USB 2000 spectrometer with a coupled integrating sphere in the range of 190 and 850nm.

The profiles of the deposits were analyzed by Veeco profiler, model Dektak 8, for obtaining the surfaces roughness.

3. Results and discussion

Manganese dioxide adsorbs ions of metals in a solution. Also, it undertakes the role of a cathode, which accepts electrons, and which consequently acts as an oxidizing agent. On the

other hand, the surfaces of the manganese chips were usually constituted by alternating the areas of oxide and metal. The predominance of any of them depends on the preparation of the surface. The proposed sequence in the process, considers this nature of metal – oxide surface as anode – cathode, respectively. Micro-electrochemical cell requires favourable ΔG, standard electrode potential, and electric conductivity in order to initiate and continue with the deposition.

Each element deposition possesses particular characteristics but then also share similarities. The deposition structures vary among each element from soft dendritic branches of silver to compact layers of aluminium or columnar grains of lead. The similarities can lead to these conditions required for deposition, such as: a) electrical conductivity between active deposition sites and the substrate, b) a higher rate of deposition than the rate of dissolution, c) a diffusion of ions on the active sites of deposition.

In the case of lead, there was no visible bubble formations associated with water electrolysis. In the case of silver, there were bubble formations and their liberation caused the lost of electrical contact between metal substrate and the active deposition sites, which particularly favoured the soft structure. In the case of aluminium, with a very low standard electrode potential, there were prolific formations of bubbles but the layers deposition prevents any significant effect.

3.1 Lead ions transformed into oxides by Electroless deposition

The process of electroless deposition of lead ions, from aqueous solution on the system manganese metal - manganese oxide, is described in this section.

Electrolytically refined manganese chips, covered with oxide (Figure 1a) or polished (Figure 1b), were either used to illustrate deposition and for comparison. Pieces of manganese metal covered with a layer of manganese oxide, formed naturally under normal environmental conditions (amorphous MnO$_2$), and pieces free of rust were immersed separately in aqueous solutions with 100 ppm of lead during 24 h and one week. The oxide layer of the piece of Mn was removed by using a SiC No. 400 grit. The solutions were kept at room temperature (25 °C) without agitation. At the end of those periods, both samples were removed from the lead solutions, which were then filtered and stored for later analysis. The substrates with deposits were analyzed by SEM.

The following analysis corresponds to deposits from solutions containing around 100ppm of lead, which depends on the surface preparation (metallic manganese or manganese oxide) or the deposition period (middle and long term; 24 h and one week).

The Figs. 2a-b show the deposit covertures after 24 h of immersion in a 100ppm lead solution of a flat Mn chip covered with oxide (Fig. 2a) and a polished Mn (Fig. 2b). These tests were conducted at room temperature (25 °C) without stirring. It was evident, during the tests, that the polished surface had a delay of around half an hour, allowing for the formation of manganese oxide clusters, which posteriorly contribute in starting deposition. Finally, there was a thicker deposit on the manganese oxide surface. The waviness in Fig 2b corresponded to original formations of the electrolytic Mn chip.
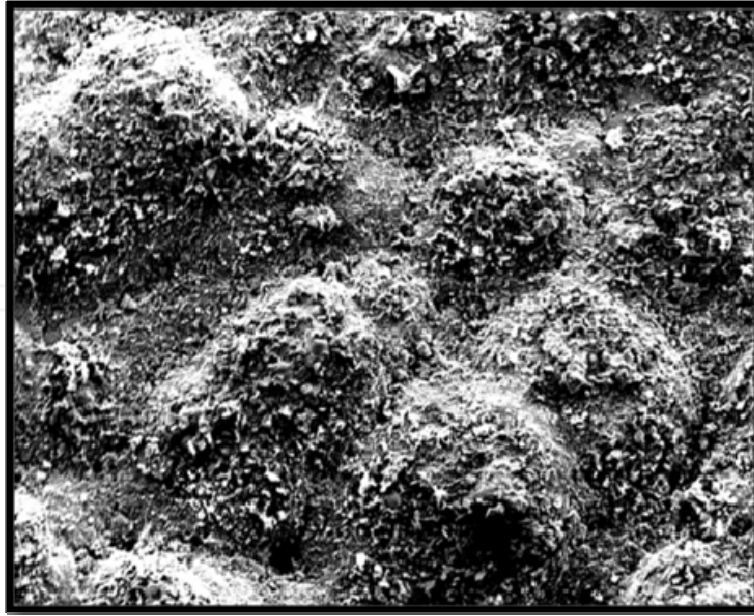
(a)
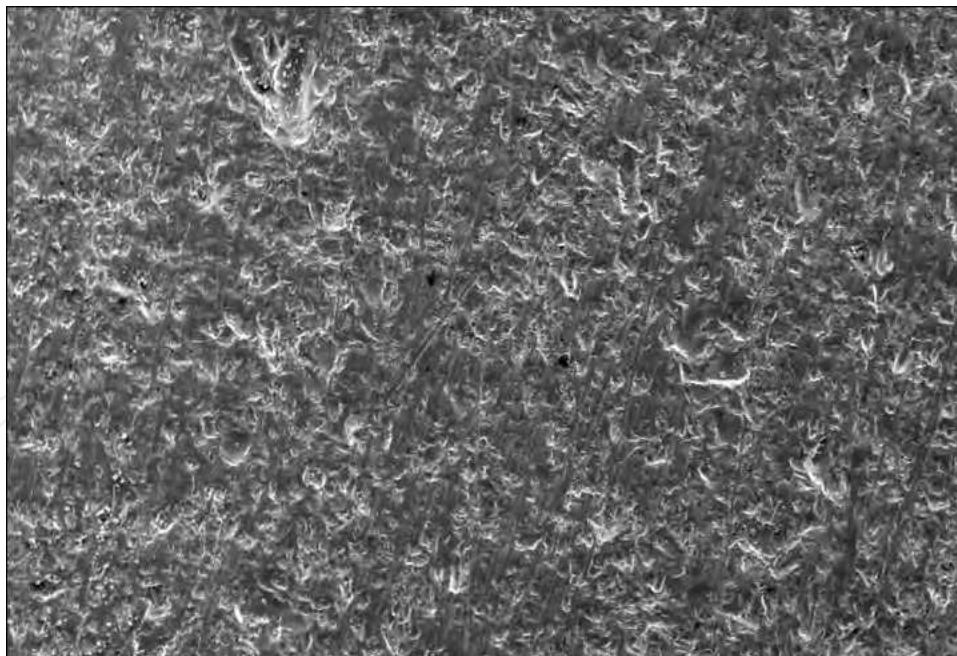
(b)

Fig. 1. **a.** SEM image using 79X of an oxide layer formed naturally on the surface of a Mn chip; **b.** SEM image using 79X on the surface of a polished Mn chip.
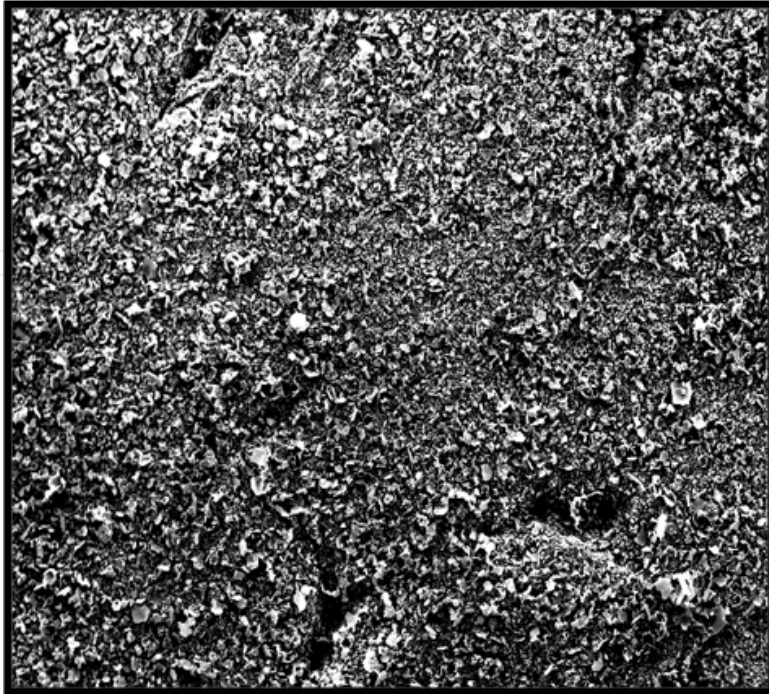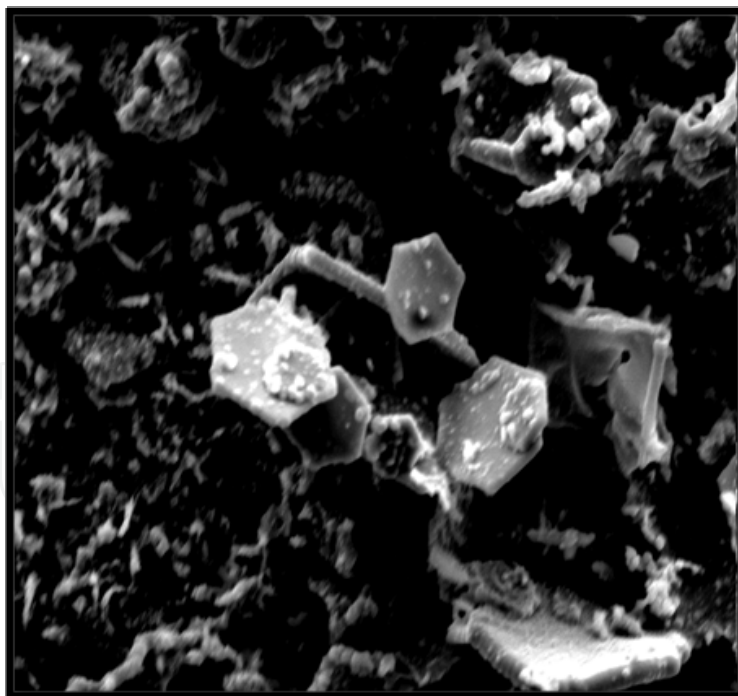
(a)

(b)

Fig. 2. **a**. SEM image, using 80X, from a flat Mn chip covered with oxide immersed in a 100ppm lead solution during 24 h.; **b.** SEM image, using 80X, from a polished Mn chip immersed in a 100ppm lead solution during 24 h.

The Mn pieces showed uniform covertures on the surface with the deposits (Fig. 3a), on which there was profuse growth. Fig. 3b shows a magnification, which resulted notorious for having frequent growths of hexagonal platelets. Along with a basis of columnar growth, there were regular hexagons with some dots on their sides. Moreover, Fig. 3b has the peculiarity of hexagonal growths on the edge of other hexagons.

(a)

(b)

Fig. 3. **a.** SEM image, using 79X, from a flat Mn chip covered with oxide immersed in a 100ppm lead solution during one week; **b.** SEM image, using 1269X, from a flat Mn chip covered with oxide immersed in a 100ppm lead solution during one week.

When analyzing the surface near the edge of the substrate, shown in Fig. 4, there were columnar formations made of numerous granules that resembled dendrites. Those growths covered the whole surface with heights that could be visible to the naked eye. The growing rate diminishes with time. This is not only due to a decrease in lead ions concentration but mainly because electrical resistivity was increasing due to lead oxide and the increasing number of grain frontiers. This characteristic of grain pillaring was frequently observed in lead oxide deposits.
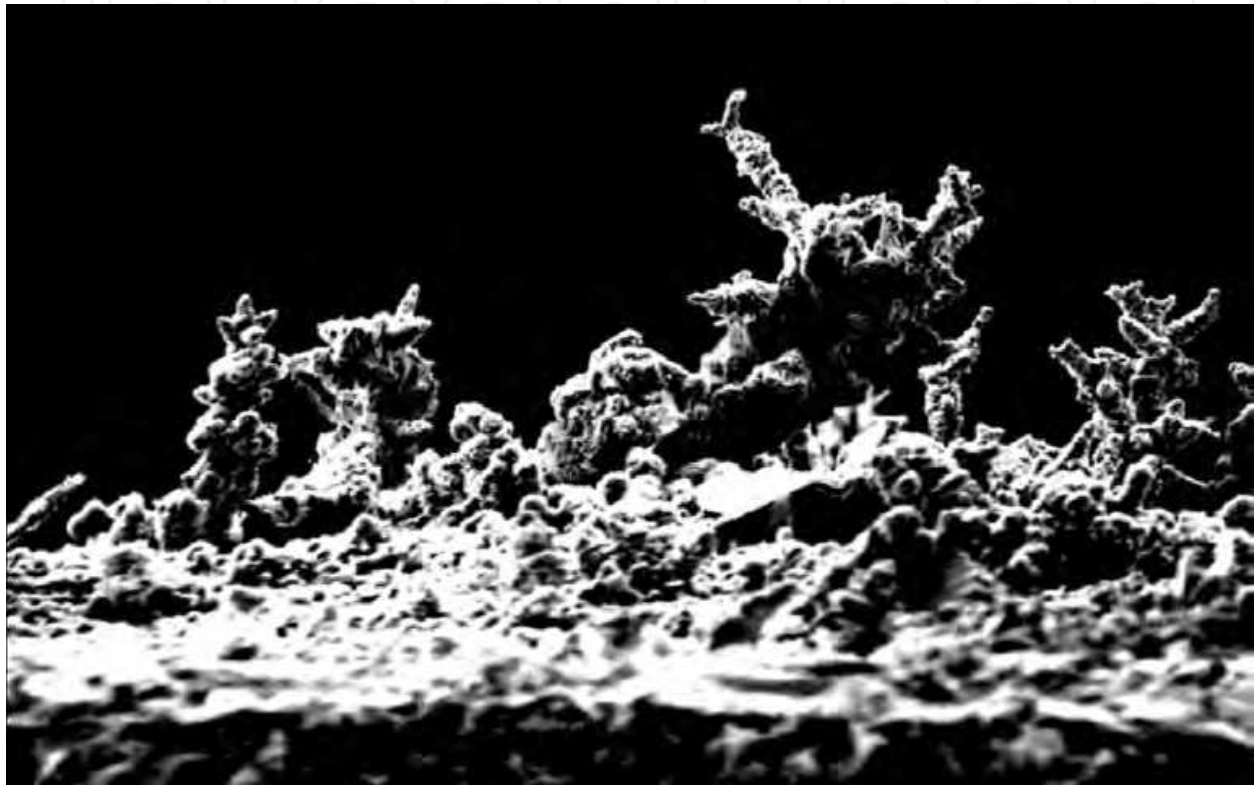

Fig. 4. SEM image, using 5077X, of dendrites stacked near an edge of the polished Mn chip.

In the non polished Mn piece, a uniform deposit was observed, on which, hexagonal lamellar formations were also present and had very symmetric profiles (Fig. 5). In the image, rod-like formations appear to be located at the center and at the left inferior corner, which were made of irregular packed granules. The rod-like formations were similar to those shown in Fig. 4 and had multiple granules which were formed concurrently through nucleation and growth.

The effect of tunneling electrons, used for imaging in the SEM, was repeatedly observed in several of the thin hexagonal platelets at Fig 5. The image shows their thickness and size were not closely associated. The electrons tunneling through hexagonal formations having translucent effect allow seeing an inner surface.

EDX analyses were conducted in both samples, polished (Fig. 6a) or covered by manganese oxide (Fig. 6b). The identified elements were: lead, manganese, oxygen and carbon. The percentages of these elements in the deposit are presented, only in an illustrative form, in Table 1.
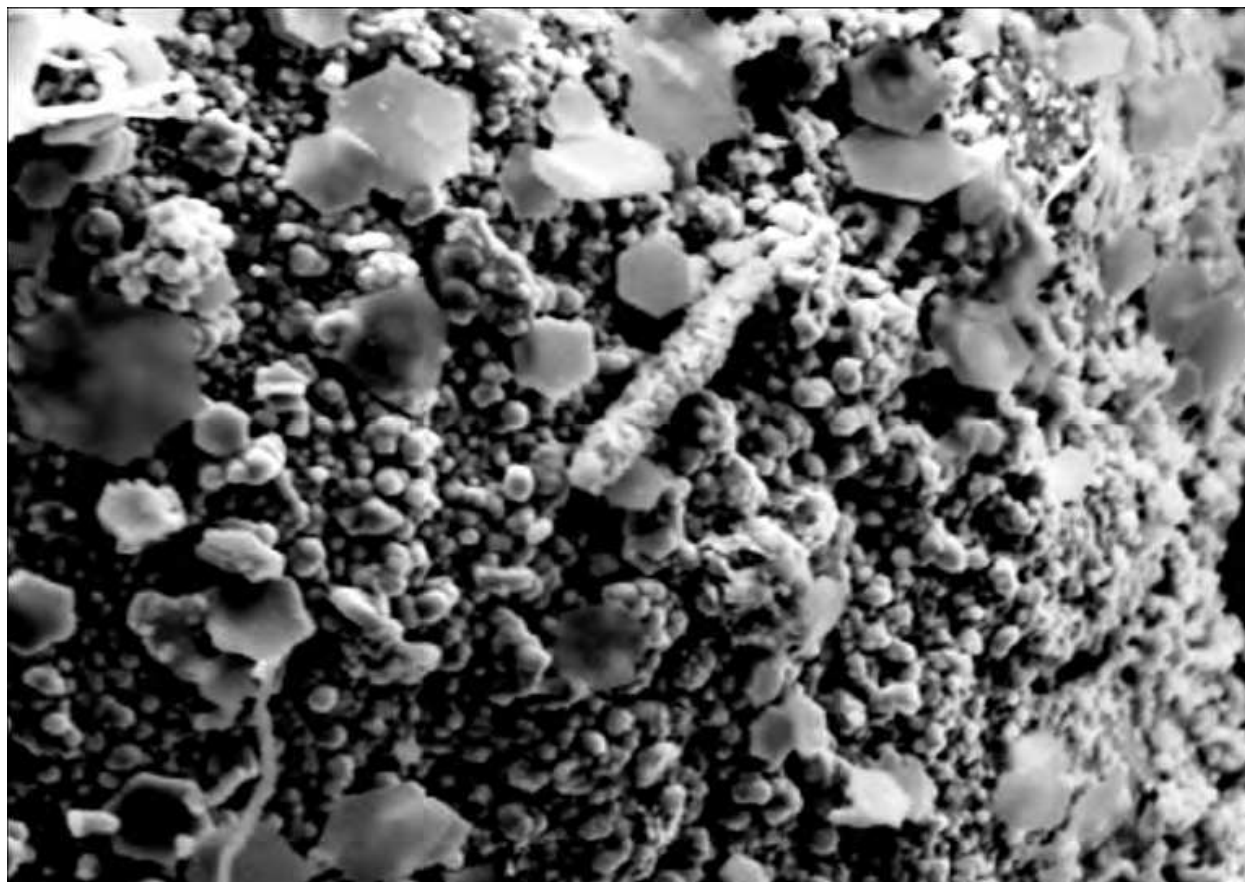
Fig. 5. SEM image at 669X from polished Mn chip immersed in the Pb solution. There were thin hexagonal formations, some of which allow transmission of the electrons from the microscope beam making them look translucent.

The EDX analysis was semi-quantitative, consequently, it is considered here illustrative of chemical composition of the deposit. The exposure to air may considerably change those compositions and change the surface appearance as manganese oxides tend to form. Considering the information from both samples, there was a close relationship between lead and oxygen content. The condition of the analyzed surfaces, there were lead oxides with manganese that eventually tended to be oxidized in the air. In other conducted experiments, lead manganese oxides tend to form ($Pb_xMn_yO_z$).

Element	Sample a (%)	Sample b (%)	Sample c (%)	Sample d (%)
Lead	52.44	39.35	37.95	1.41
Manganese	15.64	42.54	36.34	64.64
Oxygen	24.04	14.62	21.59	1.41
Carbon	7.88	3.5	4.12	4.95

Table 1. Semi-quantitative EDX percentages of elements on the surfaces: a) initially covered by manganese oxide and b) polished Mn; both during 24 h. c) Initially covered by manganese oxide and d) polished Mn; both during one week.
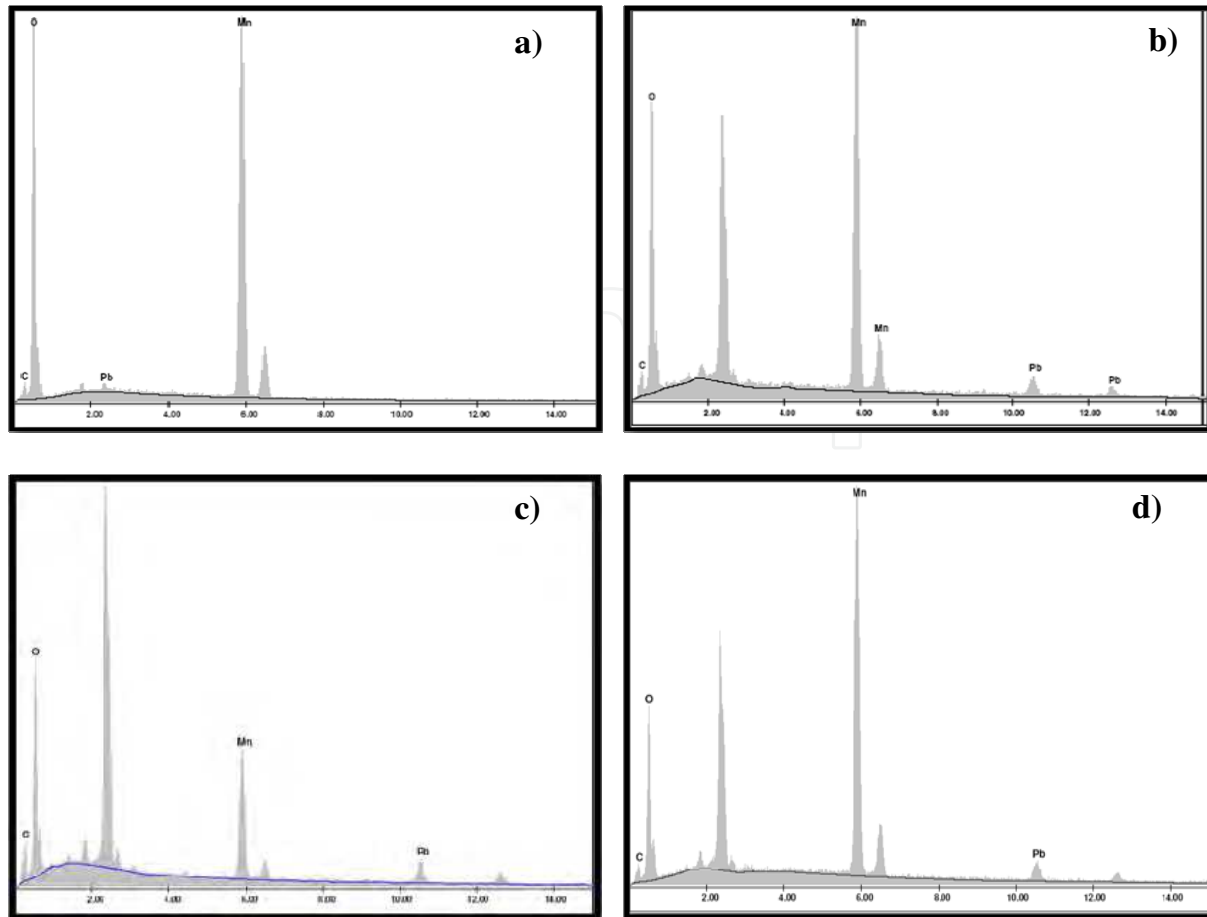
Fig. 6. EDX analysis conducted on surface: a) initially covered by manganese oxide and b) polished Mn; both during 24 h. c) Initially covered by manganese oxide and d) polished Mn; both during one week.

Table 2 presents the lead removal of samples showed after a week in contact with the solution at room temperature (25 ° C) and without agitation. ICP analysis was conducted on the solutions after the tests. There were greater depositions on Mn pieces covered by oxide than in polished Mn pieces during both periods. Also, the total lead removal after a week reached ninety percent.

The deposition was influenced by both, time and surface preparation. Nonetheless, there were other principal variables in the process: Pb concentration, the area of deposition, and the temperature. The lead deposit structure was then strong enough to apply a flow or stirring to the solution during tests. Also, this may increase the deposition rate causing a time reduction or a rise in the lead removed percentage.

X-ray diffraction analyses were conducted in order to identify the crystal composition of the deposits. The diffractograms of these samples identify a crystalline content of Pb$_5$O$_8$ (Fig. 7).

In order to observe the lead concentration influence on the structure of the deposits a 500 ppm of lead solution was used for deposits. In this series of tests, the deposition process was conducted three times, without changing the solution, but only substituting the Mn plate. Fig. 8 shows this sequence. Also, only one half of the Mn pieces were polished and subsequently

immersed in the lead solution. The immersion time for samples A and B was 24h, but sample C remained for 64h, since the formation of a deposit was not evident initially.

Time	Sample	Pb initial content (ppm)	Pb content after test (ppm)	Pb removal (%)	Area (cm²)	Pb removal (ppm$_{Pb}$/cm$_2$)
24 h	Surface covered by manganese oxide	125	115.44	7.65	0.55	92.01
	Surface of Polished Mn	125	118.45	5.24	0.58	69.73
1 week	Surface covered by manganese oxide	125	10.82	91.344	0.31	368.96
	Surface of Polished Mn	125	19.15	84.68	0.40	267.84

Table 2. Removal of Pb by Mn pieces after 24 h and one week in contact with the solution, analyzed by ICP.
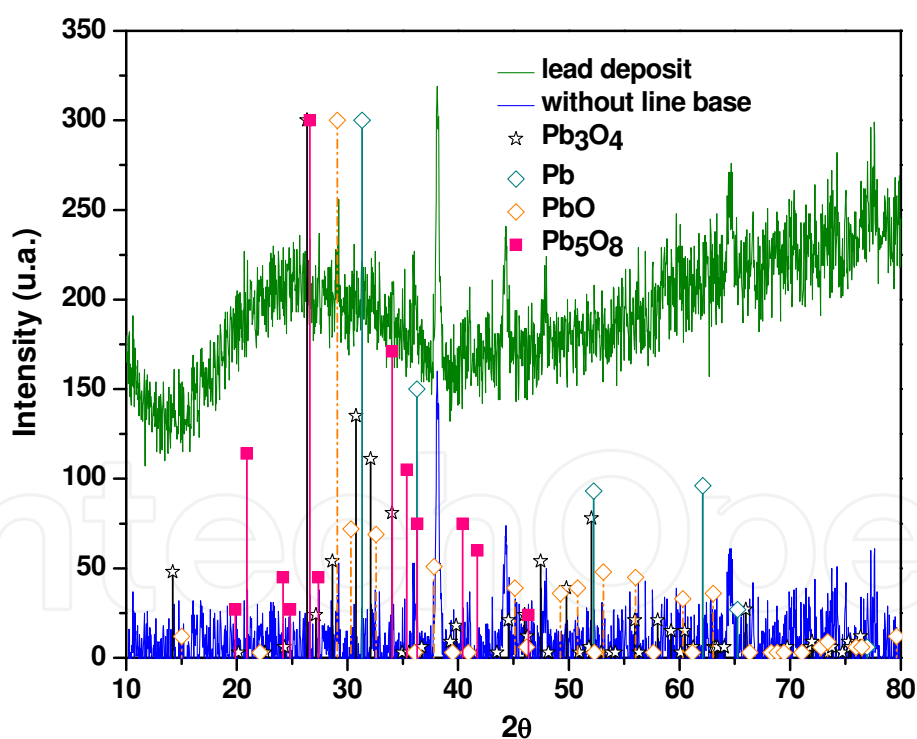

Fig. 7. X-ray diffraction of a lead deposit.

Fig. 8A shows the image corresponding to the first immersed plate into the 500 ppm lead solution A), after drying in air. The deposit was very visible and it was apparently formed by accumulations of dendrites. Under similar conditions, a second Mn plate immersed into the solution showed a still visible deposit, with thin columnar-dendritic growths and thickness (Fig. 8B). Finally, sample C showed that the deposit was present as a homogeneous

(a)

(b)

(a)

Fig. 8. a) Picture of sample A, b) picture of sample B, c) picture of sample C.

layer without a prominent accumulation on its surface (Fig. 8C). Only in the third sample there was evidence of difference between the half polished area and the oxide covered surface, which appeared as a dark area on the right hand side.

These pieces were analyzed by X-ray diffraction, which identified a predominance of Pb5O8 along with small signals indicating the presence of Pb and PbO (Fig. 9).
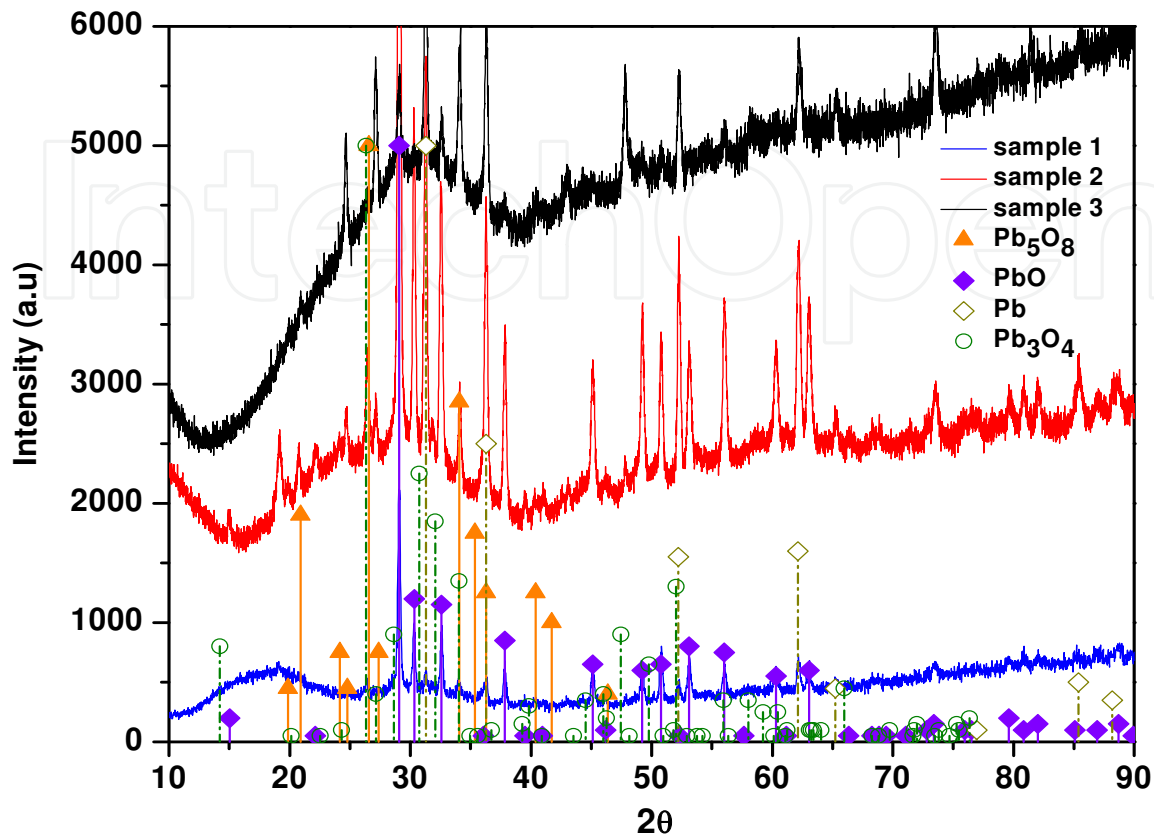

Fig. 9. Difractogram of Mn samples with deposition from a 500 ppm lead solution. A) First plate, B) second plate, C) third plate.

The kinetics of deposition of lead on manganese depends on the Pb ion concentration in solution. High concentration promotes a fast deposition and growing in a dendritic structure. The intermediate deposition rate combines semi-dendritic columns with grain nucleations. Slow deposition rates propitiate nucleations with spherical shaped grains. Nevertheless, some cases were observed with different deposition configurations.

Usually, lead deposition in the edges of a manganese substrate tended to generate the combined form of deposition. Fig 10 presents such projections from an edge of a manganese piece. It possessed a semi-dendritic column formed by grain nucleations. In this infrequent case, it was coronated by forms in a leaves-like shape.

Figure 11 shows the surface of a manganese substrate cover with a lead-based deposit after its immersion was prolonged during a month in a lead containing aqueous solution. Figure 12 shows the element EDS mapping indicating the chemical composition on surface of the lead-based deposit. The manganese covering predominantly the surface (top right). The mapping of Pb (bottom left) and O (bottom right) were more sensible to features on the surface topography. The top coverage presented an intricate needle formation. This kind of deposit covered the exposed surface of the substrate. In this case, the prolonged aging of the deposit permitted those formations as a middle point between those factors that allow the deposit and those that limited its extent.

Fig. 10. Image from a lead deposition in an edge of a manganese plate with a semi-dendritic column constituted by grain nucleations and leaves-like forms on top.

There were some factors limiting the extent of growth, such as the reduction in Pb ions concentration in solution and electric contact with the substrate. Since there were such limitations, the initial lead concentration can be reduced by increasing the area, increasing the time of contact or by successive stages of deposition.
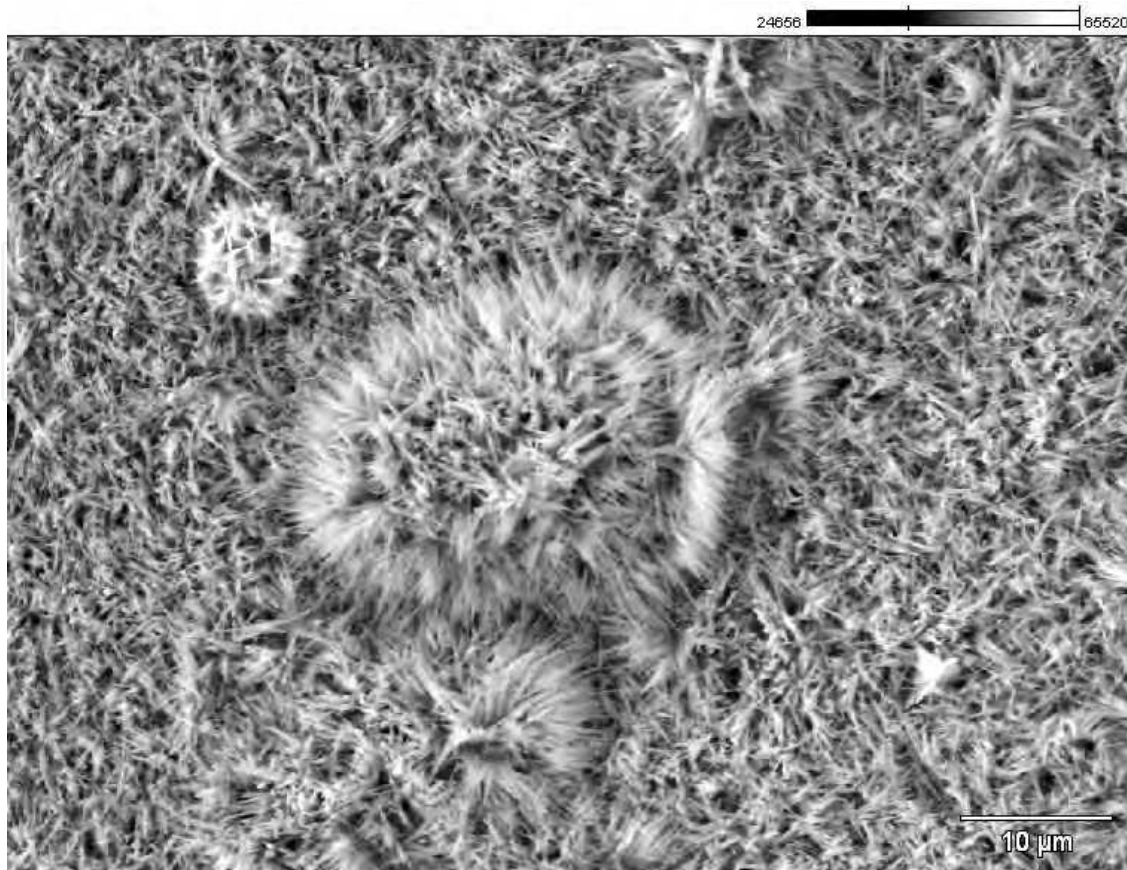
Fig. 11. SEM image of a manganese substrate covered with an intricate needle formation of a lead-based deposit after its immersion was prolonged during a month in a lead containing aqueous solution.

3.2 Electroless deposition from an aqueous solution containing Silver ions

The first step was the preparation of an aqueous solution with a silver content of 100 ppm. One half of a manganese plate was polished (grit 400), on its superior flat area, exposing a portion of the bare metal. The other half of the plaque was left with its manganese oxide which was naturally formed in air. The fundamental assumption was that there were micro-domains on the surface acting as anodes and cathodes. The purpose of this test was to discern the role that each area may play as predominantly anodic or cathodic. Both areas had oxide and metallic regions, but initializing the test in each area clearly predominated one of them.

The polished area began to be covered by a dark homogeneous layer immediately after immersion. The dendritic deposition became perceptible to the naked eye after four minutes of contact with the solution of Ag. The deposit spread to the entire surface and edges of the Mn piece after twenty minutes. The deposits initial colour was dark gray, but after seven hours, the deposit colour changed to a silvery metallic lustre. Posterior observations through a microscopy made it evident that those dendritic deposits began immediately after immersion of the Mn plate. That deposit was studied by X-ray diffraction. However, the corresponding difractogram only revealed the presence of metallic silver and it did not show any crystalline form of oxides.
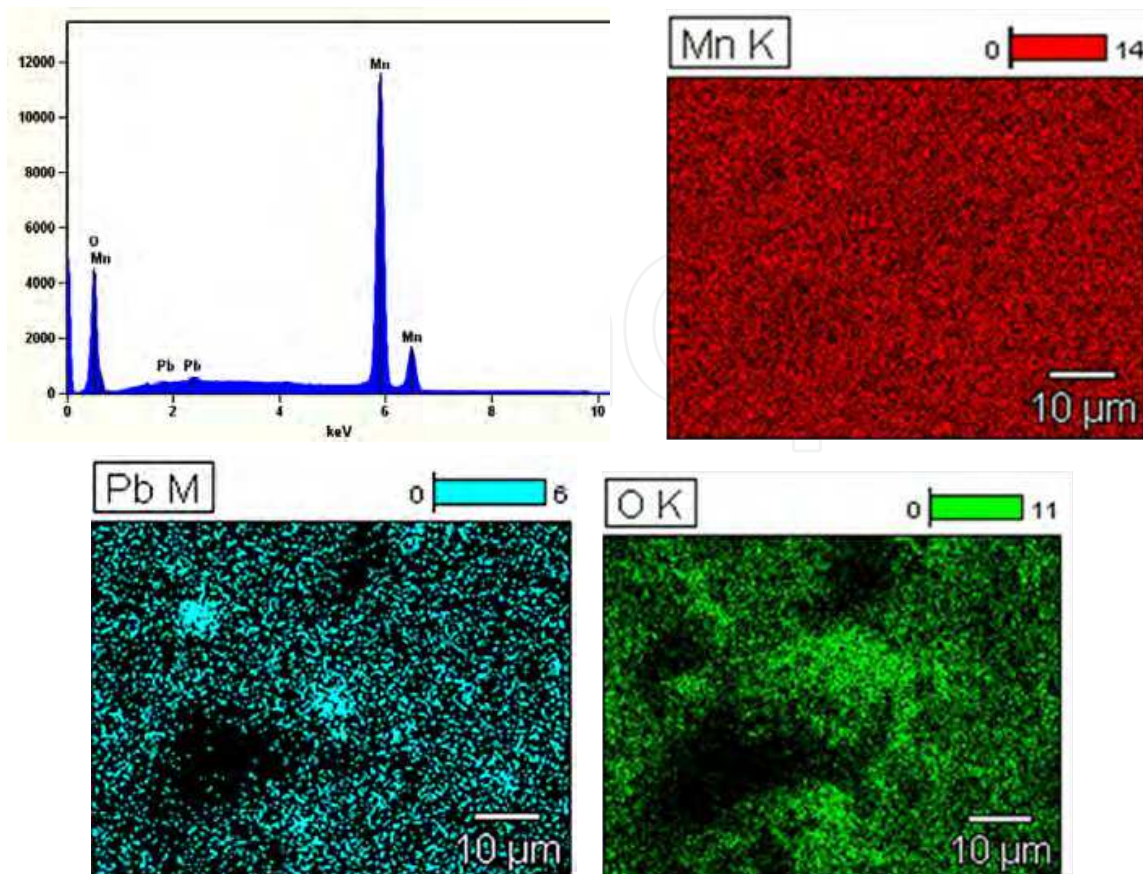
Fig. 12. EDS mapping indicating the chemical composition on surface of the lead-based deposit shown in Fig. 11. The manganese covering predominantly the surface (top right), which also contains Pb (bottom left) and O (bottom right).

The second step was the preparation of an aqueous solution with a silver content of 500 ppm. As in the previous case, one half of a manganese plate was polished and the other one left with manganese oxide.

On this occasion, as soon as the piece came into contact with the solution, the metallic part was covered with a black homogeneous deposit. Meanwhile, in the other half of the piece that still had its oxide layer a broad white spot appeared. The Mn piece was covered with a deposit of gray moss-like colour in less than a minute, which turned dark after three minutes. Five minutes after initializing the test, it was obvious that at the edges of the piece the appearance of deposit was silvery and in the form of dendrites. Throughout the whole surface, the piece was acquiring this colour.

In the case of water containing silver there were some features that differed to lead and other metals. The deposit's rate of formation is by far much faster, with a very long extent of growth, more dendritic and, hence, openly structured with small volumetric density. On the other hand, the only identified crystalline formation was metallic silver. There are two main causes for this behaviour, the standard electrode potential for silver and its electrical conductivity. The first one is related to a favourable ΔG for deposition. The second one allows the electrons transmission from the active reduction sites to the substrate. Also, under normal environmental conditions due to their electronegativity, silver patina is formed by silver sulfide rather than silver oxides.

The process of silver deposit growth showed three stages. In the first, the deposit began with a dark appearance that later changed to clearer as dark gray. In the second, it continued generating an algae or moss-like structure consisting of dendritic formations. Subsequently, the silver crystals grew into a lustrous white metallic colour in the form of dendrites with long needle-shaped branches. Those formations were projected from the sponge-like formation with extensions of around seven millimeters.

Finally, the previous stages were covered by a dendritic growth with a dark and closely packed cauliflower-like formation. This formation was extended beyond the Mn piece
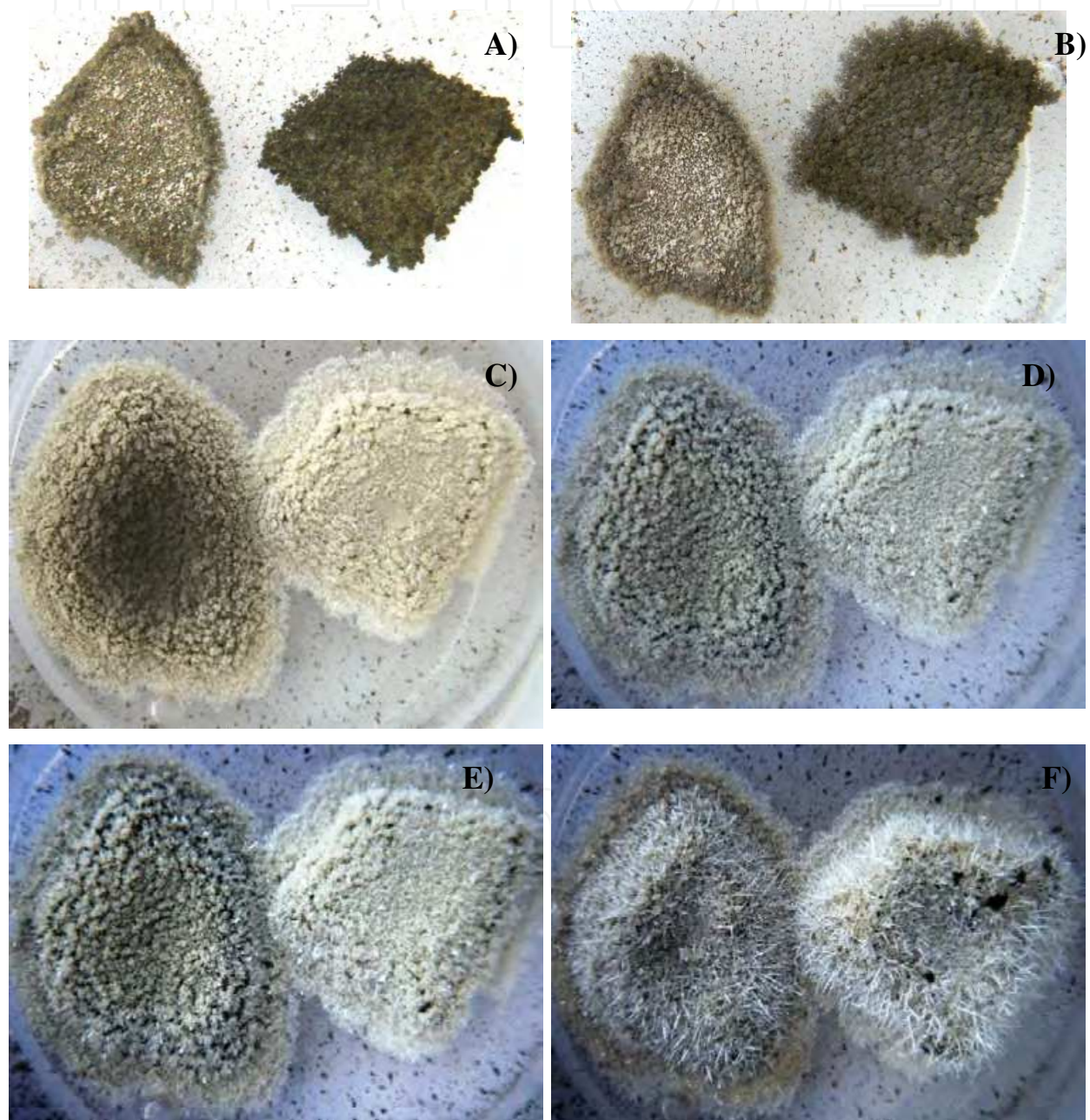

Fig. 13. Sequence of silver deposits growth on the system manganese-manganese oxide. The white appearance was a highly crystalline form of needle-dendritic silver. The dark appearance was dendritic silver.

covering the bottom of the container. Its size surpassed the original Mn piece, even reaching inches away from the substrate and was several millimeters thick. At some point, this layer reached its maximum extent but it is of low density with an algae-like formation and, with time, it increased its density and stiffness.

Fig. 13 shows the sequence of images of silver growth using two manganese pieces. The dendrites on the border of the pieces grew faster. The white appearance was due to the formation of shiny silver needles (Fig 13C). The deposition ended when bubbles, formed underneath, breaking the electrical contact between the active reduction sites and the metallic substrate. In Fig. 13F, the black spots, over the silver growths of the right piece, were the apertures made by the bubbles ejection.

The third stage was directly associated with bubble formation, which in turn may depend on the thickness of the first layer. A first thick dendritic formation may subsequently promote a rapid bubble generation. On the other hand, a first thin dendritic formation fosters the growth of crystals of silver, which started as needle-like formations but then grow in dendritic shapes. Higher concentrations may cause a short first stage, which indeed may reduce the probability of bubble formation and a corresponding abrupt interruption of the deposition. The silver ions concentration in the solution plays an important role in the kinetics of forming deposits. High concentrations and overpotentials propitiate such dendritic configurations (Herlach, 2004).

When considering the whole silver deposition process, the growth was in dendritic form, and there were different dendrite types in each stage. Upon removal of the deposition from the solution, there were two forms, an algae-like mass and long single silvery needles (some millimeters long).

Fig. 14. Another silver dendritic growth with needle-like formation. The black spots on top were holes left by the bubbles ejection.

As in the case of the previous section with lead, the dendritic growths were bigger at the borders of the Mn pieces. Also, exposing the deposits to air over the Mn piece leads to a manganese oxide coverage (Mn_3O_4). This not happened when the Mn piece was removed. In any circumstance, the silvery needles with single monocrystals appearance remained unchanged.

Figure 15 shows the status achieved by the growth of silver deposit on manganese when it is allowed to continue for several weeks without external disturbance. The same manganese piece, with a clean surface, can restart the process even in the same solution whether starting with 100 ppm or 1000 ppm. The latter contains enough silver ions to repeat the procedure several times. In the case of those silver growths, the substrate easily lost contact with the depositions. An easy cleaning of the surface made the Mn piece available for a new deposition.

Fig. 15. Two silver deposits, after a month, on Mn pieces located at the center of the formation.
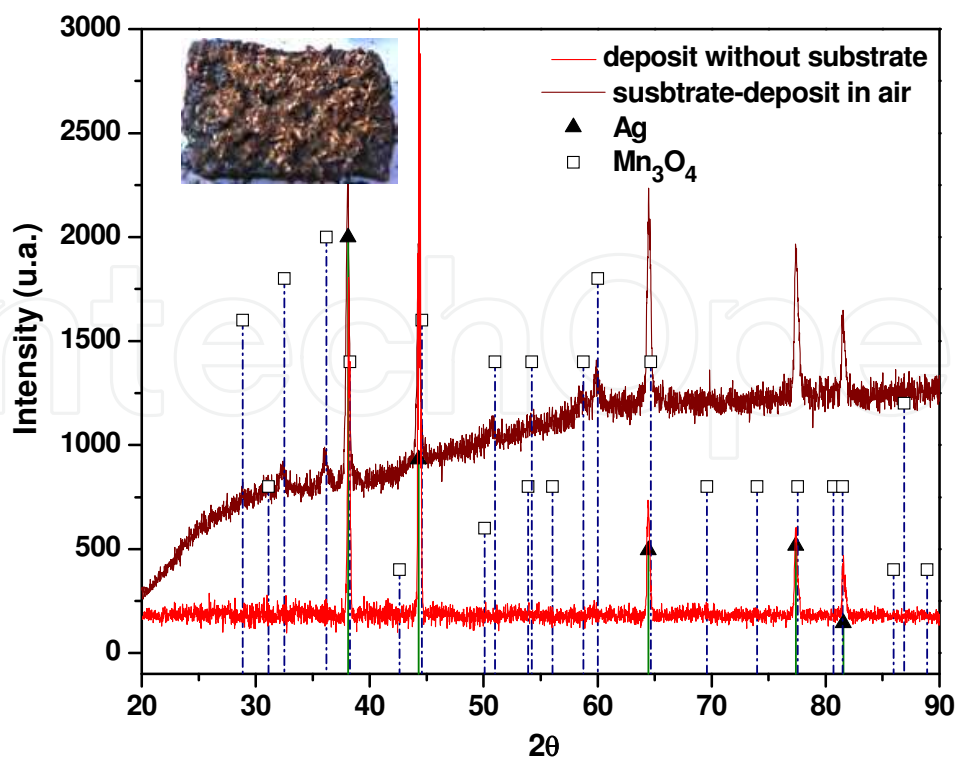
Fig. 16. Diffractograms of the bare silver deposit and on the Mn piece.

The electroless deposition process using manganese-manganese oxide usually stops by removing the metallic substrate. As mentioned previously, and similarly to the case of lead, by the exposure of deposits to air that remained on the substrate got a Mn$_3$O$_4$ coverage (Fig. 16 – inserted picture). Fig. 16 shows the diffractograms of a sample with and without the Mn substrate. The coverage of the deposits by a manganese oxide changes the shiny silver finish to a brownish colour, which happened in a matter of minutes. The reason for this change was not associated to a reaction of the silver with environmental sulfur, which usually constitutes the dark patina (Ag$_2$S).

On the other hand, if the silver deposit lost contact with the manganese substrate, a manganese oxide layer was not formed. This behaviour seems related to a Mn migration to the outer surface, which was interrupted. These are explained by redox reactions that require the transfer of electrons between the surface where oxidation takes place and the cathode, where deposits grew. Figures 13 and 14 show the deposited material corresponding to the three stages of the deposit, where highlighted the prominent needles and the foamy material generated in the third stage. A simply water cleaning allowed appreciate the state of the manganese surface with few firmly attached material.

From those tests, we can infer that Mn metal parts with its oxide may result with the potential for water remediation as well as for recovering some precious metals.

3.3 Electroless deposition from an aqueous solution containing Aluminum ions

In the study of a manganese-manganese oxide surface, immersed into an aluminum ion solution, a distinctive dense deposit, nearly continuous and homogeneous, was obtained. In this case, the deposit did not present dendritic formations and a high number of bubbles were formed on the surface. The proposed explanation refers to the potential difference between the areas acting as anodes and cathodes, which had favourable results the potential water electrolysis forming hydrogen and oxygen on the substrate.

The kinetic was fast using a solution with 500 ppm of aluminum. It was possible to observe a deposit and bubbles few seconds after immersion. However, the deposition rate decreased faster possibly attributed to two facts: a) the bubbles covering the surface (each measuring up to 2mm in diameter) and b) a thick and viscous layer of hydroxides forming above the surface. In order to permit deposited layer growth, some physical methods were used such as: a) magnetic stirring, b) ultrasound, or c) direct friction with other surface. Those methods were effective to displace both, the bubbles and the hydroxides. This procedure was contrary to the requirements in the previous case for silver deposition.

The deposited layer became perceptible through colour changes on the surface. The substrate acquired a lustrous golden metallic tonality, which appeared homogeneously and was perceptive to the naked eye and cameras without amplification. This effect was attributed to the interference of the light reflecting on the surface due to the thickness of the layer and its refraction index. Subsequently, as the layer became thicker, the surface took a lustrous metallic white tone.

The deposit from an aluminum containing solution did not show dependence on the initial surface condition, regardless of starting with a polished or oxide surface. Also, it differed from silver and lead susceptibility to a cover of manganese oxide. The final cleaned surface remained unchanged when exposed to air for long periods.
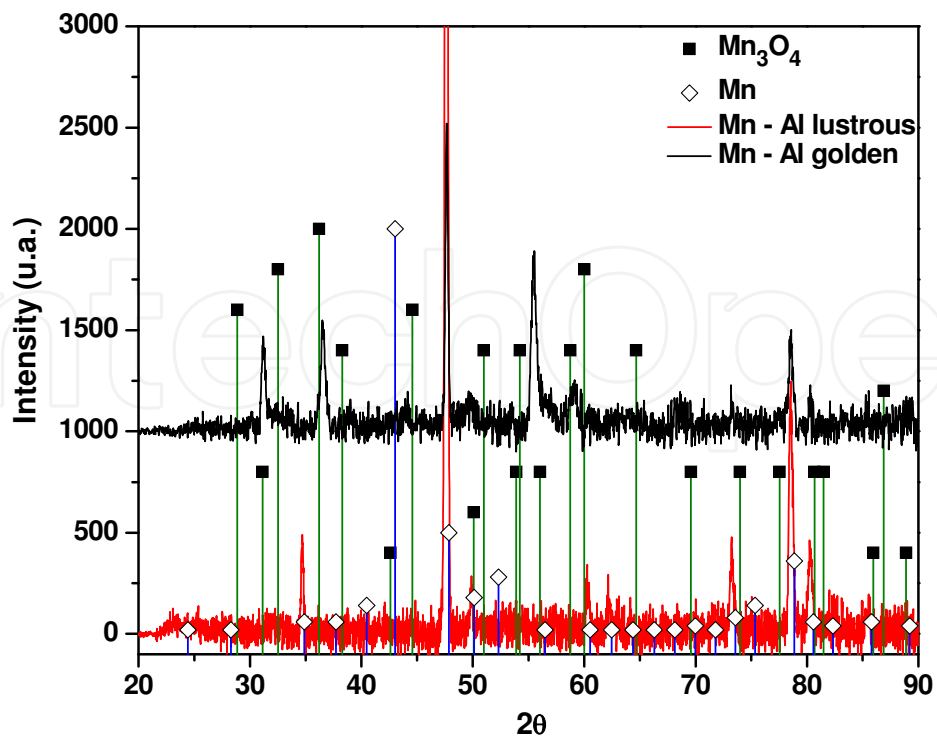
Fig. 17. Difractogram of aluminum deposit on manganese substrate.

Fig. 18. Aluminum deposits on manganese at different times in the process. The white metallic finishing remained unchanged with exposition to air.

The x-ray diffraction analysis of deposits, from an aluminum containing aqueous solution, did not allow the identification of the metallic aluminum phase. Fig. 17 shows a diffractogram that identifies only the manganese metallic substrate and, in some cases as this one, Mn$_3$O$_4$. Presumably, the X-ray diffraction was not able to identify the aluminum due to the small thickness of the layer.

The Fig. 18 shows the deposition from a solution containing aluminum on manganese substrate at different time during the process. It is possible to observe the bubbles forming on the substrate with a metallic deposit appearance.

Fig. 19 shows a SEM micrograph of the Aluminum deposit using 1000X (the scale bar indicate 25μm). The first notorious characteristic of this kind of deposits is a flat surface devoid of dendritic growths. An EDS microanalysis shows Mn, O and Al on surface. The signals for Aluminum and oxygen were very weak. The semi-quantitative calculus was: Oxygen 1.71wt% (5.6 atom%), Aluminium 0.42 (0.82 atom%) and Manganese 97.87 wt% (93.58 atom%). This can be attribute to a thin layer of Aluminum deposit, as in the case of the difractogram. The composition distribution maps on surface corresponding to Al, O, and Mn, respectively. There was a small distribution of Aluminum detected on surface.
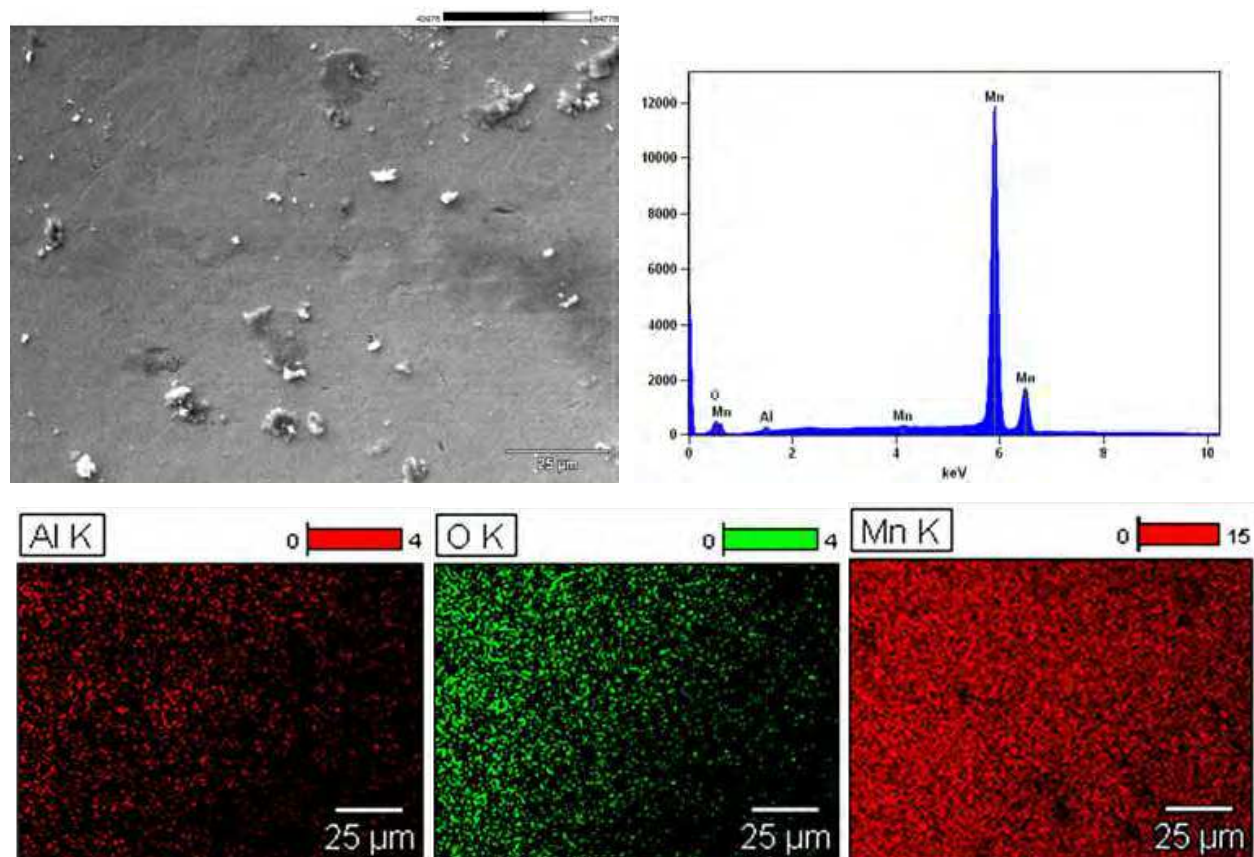

Fig. 19. SEM micrograph of the Aluminum deposit using 1000X (the scale bar indicate 25μm). Also, EDS microanalysis shows Mn, O and Al on surface. In the second line, the composition distribution maps on surface corresponding to Al, O, and Mn, respectively.

The Figure 20a shows the absorbance and reflectance spectra for a deposit from an aluminum solution on a manganese-manganese oxide substrate. The spectrum of the substrate is presented in order to compare the effect of the aluminum deposit on the absorbance and

reflectance. In black, associated with the left **y** axis, the reflectance is shown. Correspondingly, associated with the right **y** axis, the absorbance is shown. The band presented in the reflectance spectrum for the bright aluminum deposit corresponds to the lamp used for illumination. Despite having used of an integration sphere in contact with the sample surface, the sample maintains a difference in reflectance in relationship to the reference that causes a lamp spectrum replication. Additionally, in Figure 20b, it is possible to quantify the surface appearance with the chromaticity diagrams.

Table 3 shows the color parameters, according to CIE (Commission Internationale de l'Eclairage): lightness (L*), red-green (a*) and yellow-blue (b*). The dominant wavelength is included, which evoke colour perception as given by a complicated light mixture. The purity perceived was thought to be in the range of 0-1 from white illumination to pure colour.
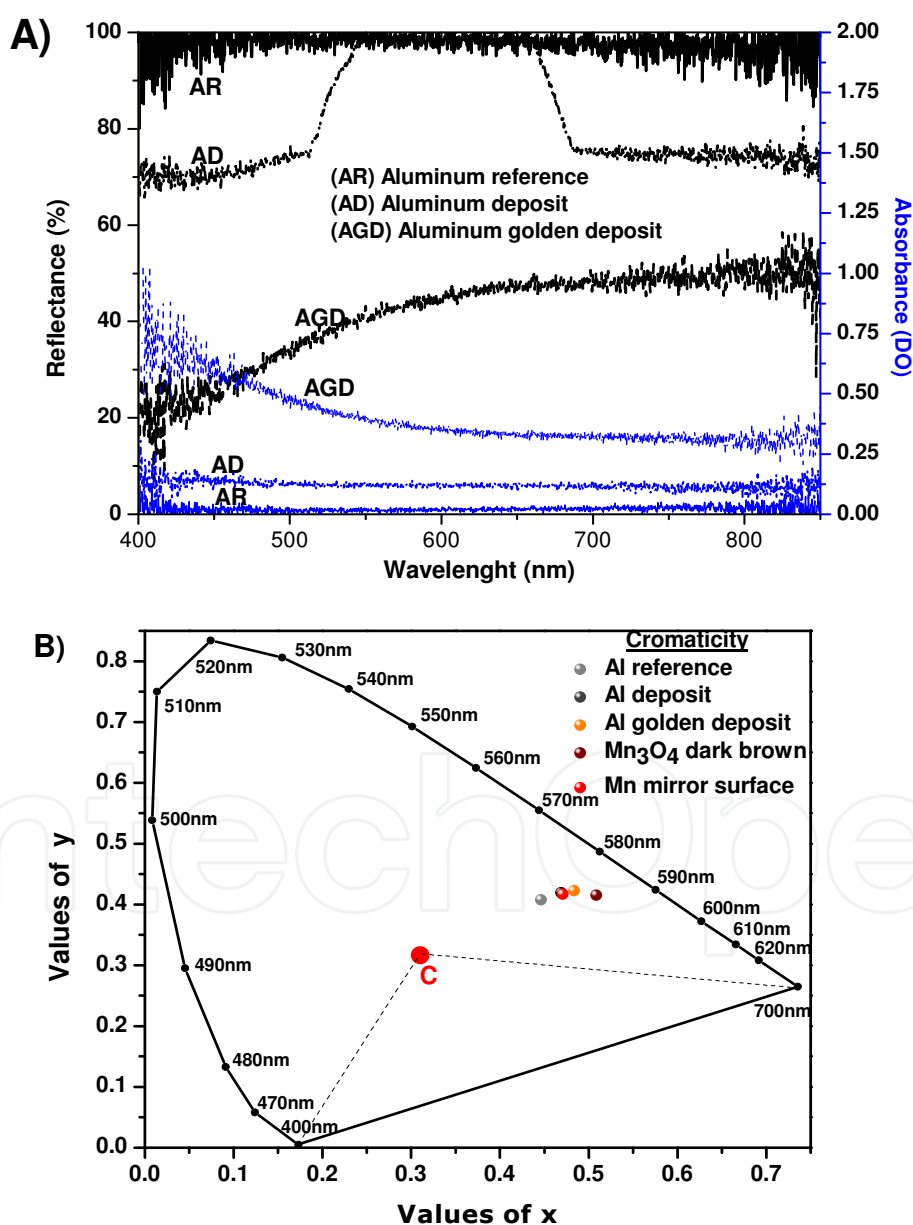

Fig. 20. A) Absorbance and reflectance spectra for the aluminum deposit. B) Chromaticity diagram for five samples of aluminum deposits.

Using Figure 20 and Table 3, it is possible to evaluate the obtained deposit finishing. It was possible to observe a bigger difference comparing the deposit and a manganese-manganese oxide substrate, which had a dark brown color. On the other hand, the bright deposit obtained was brighter than the deposit on the polished manganese.

The aluminum deposits on manganese- manganese oxide have a high reflectance. The profilometry analyses allowed quantify the surface roughness.

The images in Figure 21 were acquired by a video camera integrated to the profilometry apparatus, in the magnification range up to 70. A white LED was used as an illumination

	Aluminum	Al bright Deposit	Golden deposit	Dark brawn Mn$_3$O$_4$	Mn polished
CIE L*	99.5	98.4	76.2	44	97
CIE a*	-0.5	3	5.5	9.5	4.5
CIE b*	-0.4	18.1	22.9	20.6	17.2
λ $_{dominant}$ (nm)	583.0	580.6	589.3	595.0	589.2
purity	0.014	0.231	0.352	0.478	0.226

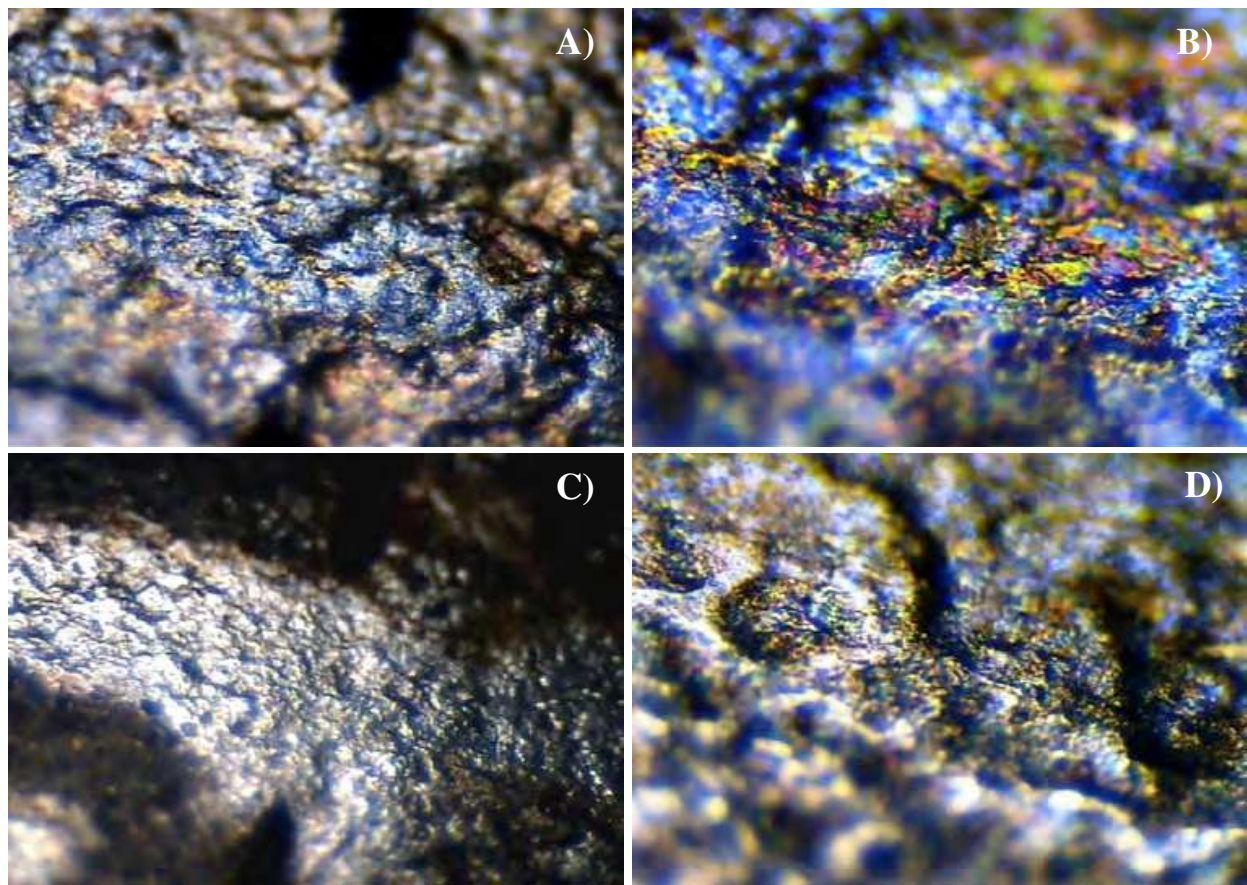Table 3. Colour parameters for the five samples represented in Figure 16B.

Fig. 21. Images of aluminum deposit on manganese-manganese oxide. A) and B) corresponds to a deposit on mangense-manganese oxide as susbtrate at 70 and 700x, respectively; C) and D) corresponds to a deposit on manganese with an ititially polished surface at 70 and 700x, respectively.

source which was put at the opposite side of the camera. It was possible to observe only specular light reflecting on surface (according to reflexion law).

Fig. 21 shows marked irregularities on the surface of deposits from an Al containing solution. This kind of surface is characteristic for aluminum deposit in contrast to the silver and lead dendritic deposits.

Table 4 shows the average roughness (Ra), the standard deviation (Rq), the number of peaks (Pc) and the distance between peaks (Sm). For references, the values for manganese substrate polished (using SiC #600) and a manganese-manganese oxide are presented. The measurements of aluminum surfaces are presented duplicated (A and B), the number (1) refers to the aluminum deposit on manganese-manganese oxide substrate and (2) refers to the polished manganese substrate. The unit of Ra or Rq is Armstrong. Pc shows, in those cases, only bigger picks, which made a great contrast between the substrate with oxide and the other surfaces. Also, the Ra of the polished surface had a great contrast compared with the others. The roughness of the deposits possessed relatively high values.

	Mn substrate with manganese oxide	Al (1A)	Al (1B)	Mn substrate polished (600)	Al (2A)	Al (2B)
Ra	13,213	61,908	47,460	4,459	48,332	14,467
Rq	18,169	77,715	63,501	5,681	58,349	18,086
Pc	119.98	12.00	17	30.00	6.00	21.43
Sm	113	1,137	753	630	1,869	519

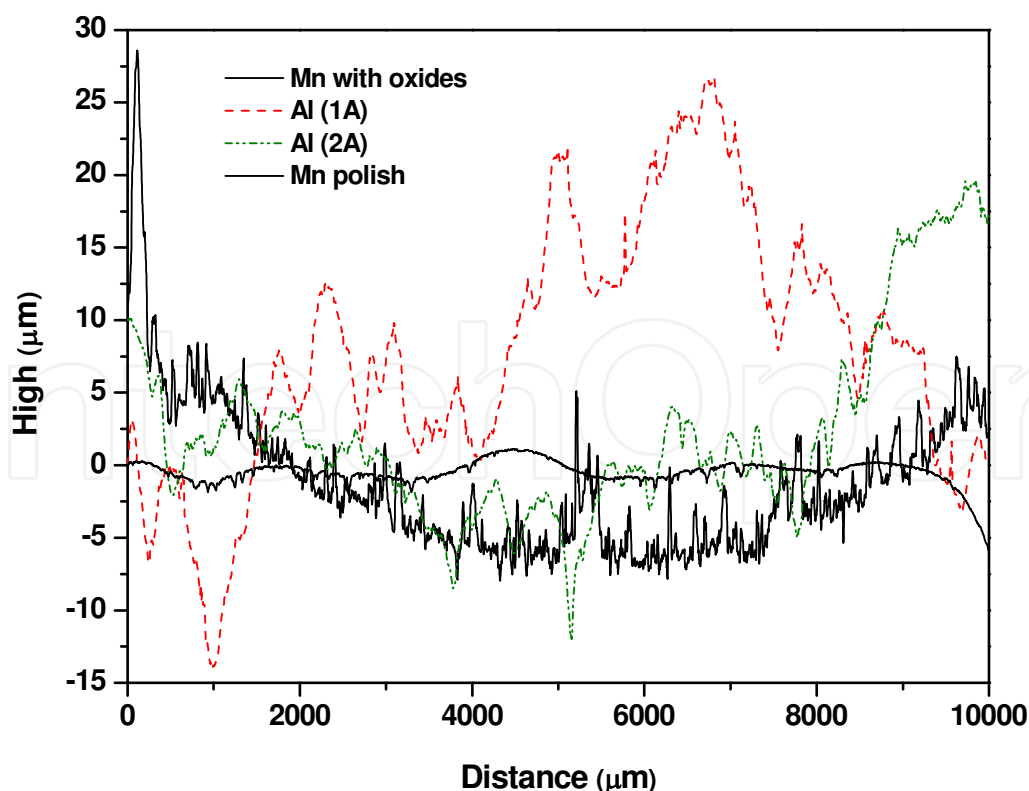Table 4. Roughness parameters profilometry obtaines for aluminun deposits.

Fig. 22. Aluminum deposits profilometry from samples starting with polished and oxide surfaces.

Fig. 22 presents the graphs associated to the Table 4. The four profilometries correspond to samples prior (continuum lines) and after (doted lines) deposition in an aluminum containing solution. The original polished surface was smooth and the one with oxide had a roughness characteristic to it. After deposition, Al 1A that corresponds to a surface with oxide had wide and high picks. Meanwhile, Al 2A had a slightly inferior roughness.

4. Conclusion

This work has addressed the issue of water treatment contaminated with metal ions by deposition using the system manganese-manganese oxide. The research identified the case as a new alternative for water treatment and even the concentration of noble metals. Through the use of manganese-manganese oxide, electroless depositions were achieved for three cases under study: lead, silver and aluminum. Those deposits range from the fast dendritically structured silver with metallic crystals; passing through the lead oxides mixing with dendrites, hexagonal platelets and nucleations; and the extremely negative standard electrode potential of aluminum, which possessed a highly reflective layered growth.

Unlike the limited manganese oxides capacity for metal adsorption, the system manganese-manganese oxide promotes redox reactions leading to a massive deposition. Basically, the process continued as long as ions in solution and electrons transfer were kept. In the case of lead, the reduction of the deposition rate was closely related to the electrical conductivity drop due to growing oxide and the multiple grain frontiers between the active sites and the substrate.

After deposition and with exposure to air, a notorious effect was that the deposition growths were covered by Mn$_3$O$_4$.

5. Acknowledgements

6. References

Dries, J., Bastiaens, L., Springael, D., Kuypers, S., Agathos, S. N., & Diels, L. (2005). Effect of humic acids on heavy metal removal by zero-valent iron in batch and continuous flow column systems. *Water Research*, Vol. 39, pp. (3531–3540)

Herlach D. D., Funke O., Phanikumar G. & Galenko P., (2004), Rapid dendrite growth in undercooled melts: experiments and modelling. In: *Solidification Processes and Microstructures*. Eds: M. Rappaz, C. Beckermann, R. Trivedi. Warrendale, pp. (277-288), Wiley, Pennsylvania, USA

Kishimoto, N., Iwano, S. & Narazaki, Y. (2011) Mechanistic Consideration of Zinc Ion Removal by Zero-Valent Iron. Water Air Soil Pollut, pp. (1-7), DOI 10.1007/s11270-011-0781-1Kontyi, o.I., Zozulya, G.I., Kurrilets, O.G. (2007). Cementation of gold by Magnesium in Cyanide Solutions, Russian Journal of Non-Ferrous Metals, Vol. 48, No. 6, pp. (413-417). ISSN 1067-8212.

Noubactep, C. (2010). Elemental metals for environmental remediation: Learning from cementation process. Journal of Hazardous Materials. Vol. 181, pp. (1170–1174)

Noubactep, C. (2009). An Analysis of the evolution of reactive species in Fe0/H2O systems, Journal of Hazardous Materials, Vol. 168, pp. (1626-1631)

Oh, B., Lee, J., & Yoon, J. (2007). Removal of contaminants in leachate from landfill by waste steel scrap to converter slag. Environmental Geochemistry and Health, Vol. 29, pp. (331–336).

Peng, K., Yan, Y., Gao, S., Zhu J. (2003). Dendrite-Assited Growth of Silicon Nanowires in Electroless Metal Deposition, Advance Functional Materials, Vol. 13, No.2, (February, 2003), pp. (127-132).

Zouboulis, A. I., Lazaridis, N. K., & Grohmann, A. (2002). Toxic metals removal from waste waters by upflow filtration with floating filter medium. I. The case of zinc. Separation Science and Technology, Vol. 37, pp. (403–416)

Recent Trend in Electrochemical Science and Technology
Edited by Dr. Ujjal Kumar Sur

This book titled "Recent Trend in Electrochemical Science and Technology" contains a selection of chapters focused on advanced methods used in the research area of electrochemical science and technologies; descriptions of electrochemical systems; processing of novel materials and mechanisms relevant for their operation. This book provides an overview on some of the recent development in electrochemical science and technology. Particular emphasis is given both to the theoretical and the experimental aspect of modern electrochemistry. Since it was impossible to cover the rich diversity of electrochemical techniques and applications in a single issue, the focus is on the recent trends and achievements related to electrochemical science and technology.

How to reference

In order to correctly reference this scholarly work, feel free to copy and paste the following:

José de Jesús Pérez Bueno, and Maria Luisa Mendoza López (2012). Novel Electroless Metal Deposition - Oxidation on Mn – MnxOy for Water Remediation, Recent Trend in Electrochemical Science and Technology, Dr. Ujjal Kumar Sur (Ed.), ISBN: 978-953-307-830-4, InTech, Available from:
http://www.intechopen.com/books/recent-trend-in-electrochemical-science-and-technology/novel-electroless-metal-deposition-oxidation-on-mn-mnxoy-for-water-remediation

INTECH
open science | open minds